Article

Ru-Catalyzed Migratory Geminal Semi-Hydrogenation of Internal Alkynes to Terminal Olefins

Lijuan Song, Qiang Feng, Yong Wang, Shengtao Ding, Yun-Dong Wu, Xinhao Zhang, Lung Wa Chung, and Jianwei Sun

J. Am. Chem. Soc., **Just Accepted Manuscript** • DOI: 10.1021/jacs.9b09658 • Publication Date (Web): 09 Oct 2019

Ru-Catalyzed Migratory Geminal Semi-Hydrogenation of Internal Alkynes to Terminal Olefins

Lijuan Song,[†,⊥,‡] *Qiang Feng,*[#,‡] *Yong Wang,*[#] *Shengtao Ding,*[#] *Yun-Dong Wu,*[†,§,¶] *Xinhao Zhang,*[†,¶] *Lung Wa Chung,*[∥,*] *and Jianwei Sun*[#,*]

[†] Lab of Computational Chemistry and Drug Design, State Key Laboratory of Chemical Oncogenomics, Peking University Shenzhen Graduate School, Shenzhen 518055, China

[#] Department of Chemistry, The Hong Kong University of Science and Technology, Clear Water Bay, Kowloon, Hong Kong SAR, China

[∥] Department of Chemistry and Shenzhen Grubbs Institute, Southern University of Science and Technology, Shenzhen 518055, China

[¶] Shenzhen Bay Laboratory, Shenzhen 518055, China

[§] College of Chemistry, Peking University, Beijing 100871, China

[⊥] Institute of Organic Chemistry, Justus Liebig University, Heinrich-Buff-Ring 17, D-35392 Giessen, Germany

Abstract

Semi-hydrogenation of alkynes to alkenes represents a fundamentally useful transformation. In addition to the well-known cis- and trans-semi-hydrogenation, herein a geminal semi-hydrogenation of internal alkynes featuring 1,2-migration is described, which provides new access to the useful terminal vinylsilanes. This process also presents a new mode of reactivity of silyl alkynes. With the proper choice of the cationic [CpRu(MeCN)$_3$]PF$_6$ catalyst and a suitable silyl group, both aryl- and alkyl-substituted silyl alkynes can participate in this highly efficient gem-selective process. Furthermore, dedicated condition optimization also allowed switching of selectivity from gem to trans by using a combination of parameters, including the suitable silyl group, additive and H_2 pressure. A systematic DFT study on the reaction mechanism revealed that the formation of the gem-H_2 Ru-carbene might be the key intermediate in both gem- and trans-addition reactions, rather than the Ru-vinylidene intermediate. The DFT results were further supported by carefully designed control experiments. This uncommon gem-addition combined with 1,2-silyl migration in the metal-carbene intermediate should open up a new synthetic avenue for alkyne transformations.

Introduction

Semi-hydrogenation of alkynes to form alkenes represents a fundamentally important transformation in organic synthesis.[1] For internal alkynes, such transformations involve stereoselectivity control, i.e. *cis*- or *trans*-hydrogenation (Scheme 1). As a textbook reaction, *syn*-selective semi-hydrogenation to form *Z*-alkenes has been well-established and found wide applications using various metal catalytic systems (both homogeneous and heterogeneous), with the Lindlar catalyst being most widely used (Scheme 1a).[1,2] The *syn*-selectivity can be well-controlled by the intrinsically stereodefined *syn*-hydrometallation and reductive elimination elementary steps. In contrast to *cis*-hydrogenation, *trans*-hydrogenation to form *E*-alkenes has been less straightforward.[1,3] For a long time, the synthetic community has relied on the non-catalytic approaches using dissolving metals, such as Birch reduction with NH_3 or amines, although they suffer limited functional group tolerance and low operational benignity (Scheme 1b).[1c] Nevertheless, significant progress with different catalytic systems has been achieved in the past two decades, including indirect approaches.[3-5] Among them, an elegant two-step approach involving Ru-catalyzed *trans*-hydrosilylation and mild protodesilylation, pioneered by Trost, has found wide applications in complex molecule synthesis owing to its good functional group compatibility and excellent *E*-selectivity.[4] More recently, Fürstner and co-workers have further extended this *trans*-addition system to the direct *E*-selective hydrogenation using molecular hydrogen with equally excellent functional group

compatibility and stereoselectivity, thus representing a revolution on this transformation.[5]

While both *cis*- and *trans*-semi-hydrogenations have been established, geminal (*gem*-) semi-hydrogenation of internal alkynes, which delivers H_2 to the same carbon of the triple bond with concomitant 1,2-migration of the substituent on this carbon to form terminal olefins, is an under-developed transformation (Scheme 1c).[5d] Herein, we report a new example of this type as well as the detailed mechanistic studies.

Scheme 1. Introduction to Semi-Hydrogenation of Alkynes

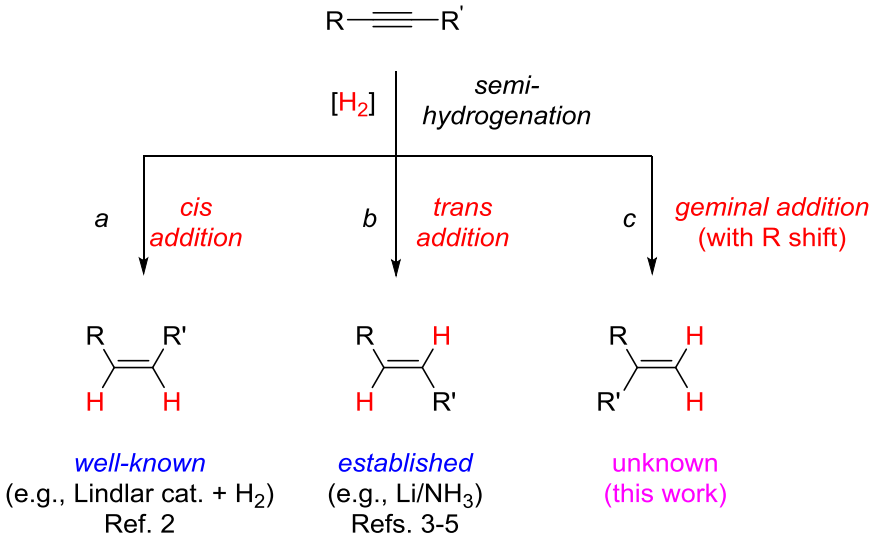

In 2013, we reported an unusual ligand-controlled regio- and stereodivergent hydrosilylation process of silyl alkynes, in which the steric difference in the ligand of the Ru-catalytic system (Cp* vs. Cp) dramatically influenced the H–Si addition mode.[6a] This remarkable selectivity divergence prompted us to explore the possibility of extending this system to stereodivergent semi-hydrogenation of silyl alkynes. To our surprise, an unprecedented *gem*-hydrogenation (Scheme 1c) was observed.

Moreover, we were also able to control the selectivity between *gem*-hydrogenation and *trans*-hydrogenation by different ligands. Mechanistically, both experimental and computational studies have excluded the involvement of a metal vinylidene intermediate, a typical pathway responsible for 1,2-migration of internal alkynes, particularly for silyl alkynes. Instead, the geminal addition of H_2 to the alkyne to form a Ru-carbene intermediate followed by 1,2-migration is more consistent to our observations (Scheme 2).

Scheme 2. Potential Intermediates Responsible for Semi-Hydrogenation of Alkynes

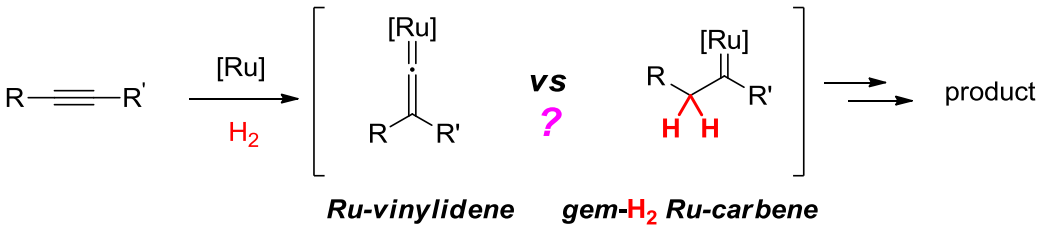

Results and Discussion

Silyl alkynes are versatile species in organic synthesis.[7] The silyl group on the triple bond not only serves as a convertible masking group, but also imposes unique steric and electronic difference (from the other terminal of the alkyne) to benefit selectivity control in the triple bond addition reactions.[6a,7] Moreover, vinyl silanes resulting from these addition reactions are useful molecules in organic synthesis and materials science.[8] Therefore, we used 1-trimethylsilylhexyne as the model substrate for our hydrogenation reaction. Initial catalyst evaluation was focused on ruthenium-

based complexes, a family of versatile catalysts for alkyne additions.[4-6,8-11] In particular, the cationic catalyst $[Cp^*Ru(MeCN)_3]PF_6$ has been superior for a wide range of alkyne additions. In many of them, particularly *trans*-hydrogenation, the Cp* ligand was noted to be necessary for high reactivity and selectivity.[5,6c,9] Unfortunately, initial evaluation of this catalyst for the hydrogenation of **1** resulted in extremely low reactivity, leading to the *E*-alkene in only 10% yield (Table 1, entry 1). A cationic Rh-complex with the same ligands did not show any catalytic activity (entry 2), nor other metal-based catalysts previously known for alkyne additions, such as $[Ir(COD)Cl]_2$ (entry 3).[6b] Inspired by our previous experience in the hydrosilylation of silyl alkynes, we believed that the severe steric repulsion might lead to the diminished reactivity when the large silyl alkyne encounters the bulky Cp* ligand.[6a] Thus, its small sibling $[CpRu(MeCN)_3]PF_6$ was evaluated.[11] Gratifyingly, at 1 bar of H_2 pressure, smooth semi-hydrogenation in DCM proceeded almost quantitatively at room temperature. Surprisingly, the reaction afforded both branched *gem*-hydrogenation product (**2**) and linear *trans*-hydrogenation product (**3**), with the former being major (B/L = 3.3:1, entry 4). While the size difference between Cp an Cp* seemed to be important, the influence of their electronic difference should not be excluded.[5f] Nevertheless, these observations foreshadowed the unusual reactivity of silyl alkynes.

Systematic optimizations were then performed in hope of improving the *gem*-hydrogenation selectivity, as this represents a new reactivity. We initially studied the influence of hydrogen pressure on selectivity. Unfortunately, at a higher pressure, the *gem*-hydrogenation pathway was disfavored (Figure 1). Next, we studied the

influence of the silyl group. Increasing its size to Et_3Si (TES), $^tBuMe_2Si$ (TBS), and $BnMe_2Si$ all led to lower reactivity and essentially no improvement on *gem*-selectivity (entries 5-7). Changing the electronic property with triethoxysilyl group shut down the reactivity completely (entry 8). However, ultimately we found that the use of phenyldimethylsilyl group ($PhMe_2Si$) led to exclusive formation of the desired branched product **2a** (B/L >30:1), albeit with low reactivity (entry 9). Then, different solvents were screened (entries 10–15), which indicated that polar and good-coordinating solvents, such as MeCN, could inhibit the reactivity. Among them, $CHCl_3$ provided the highest reactivity (entry 11). Finally, in order to accelerate the reaction, we found that the use of 10 bar hydrogen pressure resulted in excellent yield while maintaining equally high *gem*-selectivity (entry 16). In contrast to the significantly decreased *gem*-selectivity at high pressure observed with the TMS-alkyne (Figure 1), the excellent *gem*-selectivity with $PhMe_2Si$-alkyne at high H_2 pressure is remarkable, which also implies that the phenyl group in the silyl group ($PhMe_2Si$-) plays an essential role in the selectivity and deserves special study (*vide infra*). It is also worth noting that this phenyl group also makes the whole silyl group more synthetically useful regarding subsequent conversions.[12] Finally, no appreciable over-reduction to the corresponding silyl alkane was observed.

Table 1. Optimization of Reaction Conditions.[a]

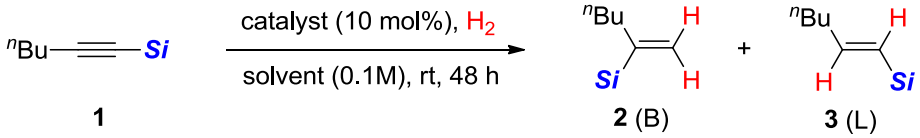

1 **2** (B) **3** (L)

entry	catalyst	*Si*	solvent	yield(%)[b]	B/L[b]
	Evaluation of catalyst				
1	$[Cp^*Ru(MeCN)_3]PF_6$	TMS	DCM	10	0:1
2	$[Cp^*Rh(MeCN)_3](SbF_6)_2$	"	"	<5	–
3	$[Ir(COD)Cl]_2$	"	"	<5	–
4	$[CpRu(MeCN)_3]PF_6$	"	"	>99	3.3:1
	Influence of the silyl group				
5	$[CpRu(MeCN)_3]PF_6$	Et_3Si	"	55	0.8:1
6	"	$BnMe_2Si$	"	22	3.6:1
7	"	TBS	"	10	<1:20
8	"	$(EtO)_3Si$	"	<5	–
9	"	$PhMe_2Si$	"	31	>30:1
	Solvent effect				
10	"	$PhMe_2Si$	DCE	41	>30:1
11	"	"	$CHCl_3$	81	>30:1
12	"	"	THF	55	>30:1
13	"	"	CH_3CN	<5	–
14	"	"	1,4-dioxane	31	>30:1
15	"	"	PhCl	78	>30:1
16[c]	"	"	$CHCl_3$	95	>30:1

[a]Reaction conditions: **1** (0.1 mmol), catalyst (10 mol%), H_2 (1 bar), solvent (0.1 M), rt. [b]Yield was determined by analysis of the ^1H NMR spectrum of the crude product using CH_2Br_2 as the internal standard. The unreacted substrate accounts for major remainder of the mass balance. [c]Run at 10 bar pressure (H_2) for 12 h.

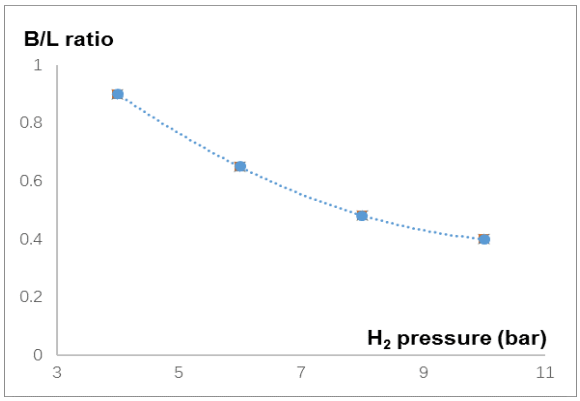

Figure 1. Dependence of B/L ratio on the hydrogen pressure. For accurate determination of the B/L ratio, TMSC≡C$(CH_2)_2$OTHP was used as substrate.

With the optimized conditions, we examined the scope of this *gem*-semi-hydrogenation (Table 2). A wide range of silyl alkynes participated in this mild process to provide a diverse set of terminal vinyl silanes with good to excellent efficiency and *gem*-selectivity. A wide variety of functional groups were tolerated, including free alcohol, ether, ester, mesylate, silyl ether, acetal, halide, and phthalimide. Electron-rich arenes, such as furan and thiophene, could also be incorporated in the substrates. Substitution of a secondary alkyl substituent, such as cyclopentyl and cyclohexyl groups, on the triple bond did not influence the high reactivity. However, with bulky ^{t}Bu-substitution, the reactivity was almost shut down. A particularly notable example is the highly electron-deficient ynone **1t**, which was equally reactive to form the corresponding *gem*-hydrogenation product **2t** with high efficiency and respectable *gem*-selectivity. It is noteworthy that the ketone carbonyl group remained intact under this reduction condition, demonstrating high

chemoselectivity as well. While this protocol is generally selective for aliphatic silyl alkynes, unfortunately, the aryl analogs failed to give high *gem*-selectivity (e.g., **2u-v**), although the reactivity remained high.

Table 2. Substrate Scope. [a]

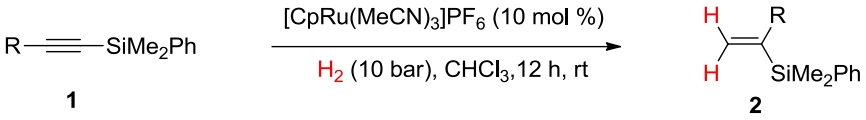

1 **2**

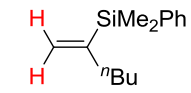

2a, 90%, B/L >30:1

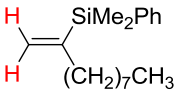

2b, 97%, B/L >30:1

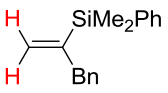

2c, 80%, B/L >30:1

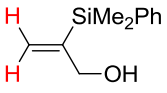

2d,[b] 85%, B/L >30:1

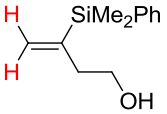

2e, 91%, B/L >30:1

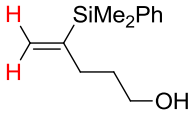

2f, 93%, B/L >30:1

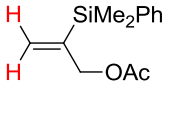

2g,[b] 87%, B/L >30:1

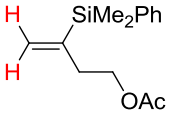

2h,[b] 99%, B/L >30:1

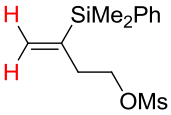

2i,[b] 95%, B/L >30:1

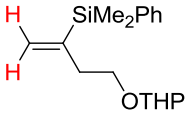

2j, 96%, B/L >30:1

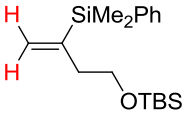

2k,[b] 92%, B/L >30:1

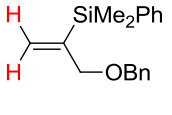

2l, 85%, B/L >30:1

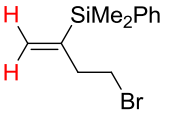

2m, 93%, B/L >30:1

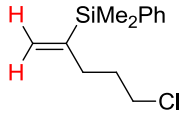

2n, 99%, B/L >30:1

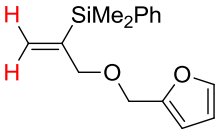

2o, 94%, B/L >30:1

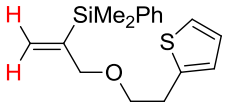

2p, 62%, B/L >30:1

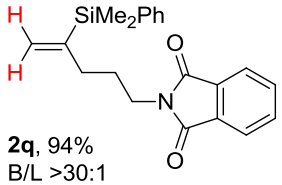

2q, 94%
B/L >30:1

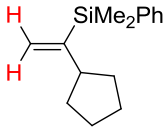

2r, 92%, B/L >30:1

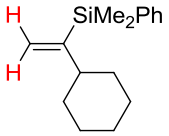

2s, 90%, B/L >30:1

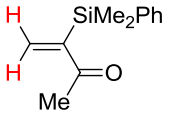

2t, 88%, B/L = 5.6:1

R = aryl:

extremely low B/L selectivity

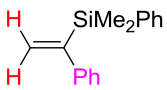

2u,[c] 95%, B/L = 1:2

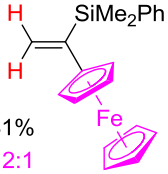

2v,[c] 81%
B/L = 2:1

[a]Reaction conditions: **1** (0.2 mmol), $[CpRu(MeCN)_3]PF_6$ (10 mol%), $CHCl_3$ (0.1 M), H_2 (10 bar), rt, 12 h. Isolated yield is provided. The B/L selectivity was determined by analysis of the ^1H NMR spectrum of the crude product. [b]Catalyst loading: 5 mol%. [c]Catalyst loading: 20 mol%.

To improve the *gem*-selectivity of aryl alkynes, we employed phenyl silyl alkyne **1u** as the model substrate for further condition optimization. Keeping in mind that the *gem*-selectivity is reversely dependent on hydrogen pressure, we first decreased the hydrogen pressure to 1 bar. As expected, the *gem*-selectivity was improved to 7:1, though at the expense of reaction time and conversion (Table 2, entry 2). We next evaluated the influence of additive. To our delight, the use of $NaBAr^F_4$ could further improve the *gem*-selectivity to 10:1 (entry 3, see the SI for more details). Furthermore, different solvents were compared, which identified DCM as the superior solvent, leading to the formation of essentially the single *gem*-isomer **2u** (B/L >30:1). The effect of additive was then further confirmed in DCM solvent (entry 6). While the origin of the additive effect is unknown, it might be related to the influence on the cationic nature of the catalyst as well as the dielectric constant of the reaction medium.

Table 3. Condition Optimization for Aryl Alkyne 1u.[a]

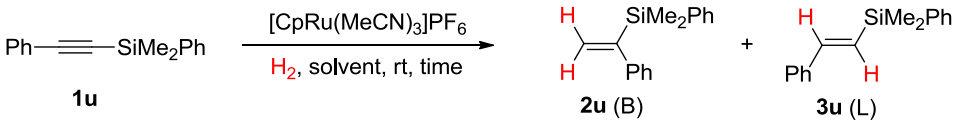

entry	additive	*P*-H_2 (bar)	solvent	time(h)	yield(%)[b]	B/L[b]
1	–	10	$CHCl_3$	12	(95)[c]	1:2
2	–	1	$CHCl_3$	25	31	7:1
3	$NaBAr^F_4$	1	$CHCl_3$	25	45	10:1
4	$NaBAr^F_4$	1	PhF	25	23	22:1
5	$NaBAr^F_4$	1	DCM[d]	48	52	>30:1
6	–	1	DCM[d]	48	18	18:1

[a]Reaction conditions: **1u** (0.05 mmol), $[CpRu(MeCN)_3]PF_6$ (20 mol%), $CHCl_3$ (0.1 M), rt. [b]Yield and B/L selectivity were determined by analysis of the ^1H NMR spectrum of the crude product using CH_2Br_2 as the internal standard. The unreacted substrate accounts for major remainder of the mass balance. [c]The conditions and data for entry 1 were taken from Table 2. [d]Run in DCM solvent at 0.05 M concentration.

With the above slightly modified conditions, we then examined the generality of this new protocol for a range of aryl alkynes. As shown in Table 4, both electron-donating and electron-deficient substituents on the *para*-position of the aryl group all led to excellent *gem*-selectivity. Unfortunately, *ortho*-substituted aryl alkynes showed extremely low reactivity, presumably due to increased steric hindrance. For electron-deficient cases, the reaction efficiency is reasonably good, although these aryl alkynes are in general less reactive than alkyl ones. In particular, the electron-rich one showed

much lower reactivity (**2aa**). We reasoned that the electron-rich arene has strong π-interaction with the cationic catalyst, thereby deactivating its catalytic activity.[13b] This is also consistent with the general observation with this type of Ru-based cationic system.[5]

Table 4. Substrate Scope on Aryl Silyl Alkynes with Improved Conditions.[a]

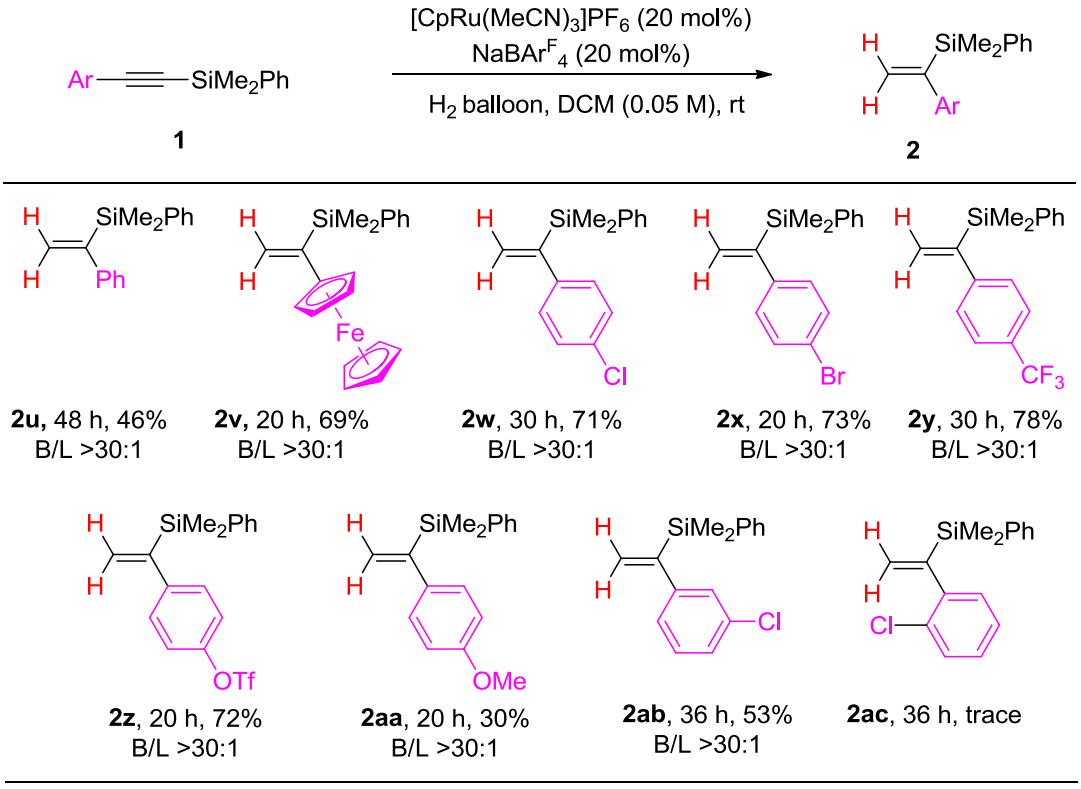

[a]Reaction conditions: **1** (0.2 mmol), $[CpRu(MeCN)_3]PF_6$ (20 mol%), $NaBAr^F_4$ (20 mol%), DCM (4 mL), H_2 (1 bar), rt. Isolated yield is provided. The B/L selectivity was determined by analysis of the ^1H NMR spectrum of the crude product.

During the study of the influence of additive on *gem*-selectivity, we found that the use of strongly coordinating ligand could reverse the selectivity. Among all the evaluated coordinative additives, we found that DABCO imposed the highest influence (see the SI for more details). After further optimization of other reaction parameters, we identified that both good yield and *trans*-hydrogenation selectivity could be obtained when the reaction of **1u** was run in $CHCl_3$ (0.05 M) at 15 bar of hydrogen pressure.

With this modification, we were able to achieve highly divergent *trans*-addition of aryl silyl alkynes (Table 5). These linear *E*-olefins were all obtained with good efficiency and selectivity, except the electron-rich ones (**3aa**), presumably due to the same aforementioned reason (i.e., electron-rich arene interaction with the catalyst).[5,13b] An aliphatic alkyne was also evaluated (entry 7). While only *trans*-addition was observed, the reaction showed moderate *E/Z* selectivity.

Table 5. *Trans*-Hydrogenation of Aryl-Substituted Silyl Alkynes[a]

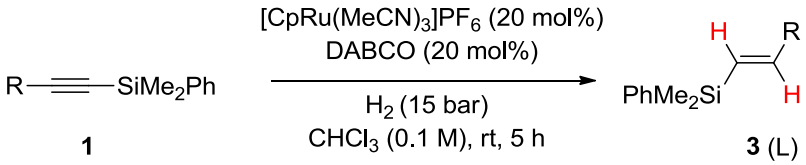

1 **3** (L)

entry	R	3	yield%	L/B ratio
1	Ph	**3u**	81	16:1
2	(*p*-Cl)C_6H_4	**3w**	73	17:1
3	(*p*-Br)C_6H_4	**3x**	75	17:1
4	(*p*-CF_3)C_6H_4	**3y**	85	>30:1
5	(*p*-OTf)C_6H_4	**3z**	78	>30:1
6	(*p*-OMe)C_6H_4	**3aa**	45	2:1
7	*n*-C_5H_{11}	**3ab**	65[b]	L only, but *E*/*Z* = 2.3:1

[a]Reaction conditions: **1** (0.2 mmol), [CpRu(MeCN)$_3$]PF_6 (20 mol%), DABCO (20 mol%), $CHCl_3$ (0.1 M), H_2 (15 bar), rt, 5 h. Isolated yield is provided. The L/B ratio was determined by ^{1}HNMR analysis of the crude reaction mixture. [b] NMR yield.

Mechanistic Studies

DFT Calculations. To understand the reaction mechanism of the novel *gem*-hydrogenation catalyzed by the cationic Ru(II) catalyst, systematic DFT (the SMD M06 method) calculations on several possible pathways were performed. Instead of the common metal-vinylidene mechanism (Scheme 2), our computational results suggest that the initial *gem*-hydrogenation process in the most favorable pathway follows the mechanism proposed for the related hydrosilylation and other hydrofunctionalizations by us[6,13] as well as by the Fürstner and Thiel groups.[5] First, the exchange of two MeCN ligands by H_2 and the alkyne substrate forms σ-H_2 Ru(II)

complex **A2** (Figure 2), followed by the rate-determining concerted oxidative hydrogen migration via **A3a-TS** with the barrier of ~25.3 kcal/mol in solution to afford σ-vinyl Ru(IV) intermediate **A4a** (ΔG_{soln} = 20.5 kcal/mol).[14] A very facile rotation along the C_α–C_β bond of **A4a** preferentially takes place to form a more stable ruthenacyclopropene intermediate **A6a$_{trans}$** (ΔG_{soln} = 13.3 kcal/mol) via **A5a-TS$_{trans}$.**[15] Interestingly, different from the hydrosilylation and other hydrofunctionalizations,[13a] this critical ruthenacyclopropene intermediate does not prefer a direct reductive hydrogen migration to the C_α atom to give the *trans*-addition product **B1** due to a higher-energy transition state **B1-TS** (ΔG_{soln} = 20.2 kcal/mol, Scheme 3). Instead, as proposed by Fürstner and Thiel groups,[5c] the ruthenacyclopropene intermediate **A6a$_{trans}$** or **A6a$_{cis}$** preferentially undergoes another novel reductive hydrogen migration to the C_β atom to give the key and quite stable Ru(II)-carbene intermediate **C2** (ΔG_{soln} = 1.6 kcal/mol) via **C2-TS1** (ΔG_{soln} = 15.5 kcal/mol), along with an isomerization step via **C1-TS** (ΔG_{soln} = 15.8 kcal/mol)) or via **C2-TS2** (ΔG_{soln} = 15.4 kcal/mol). Therefore, these results show that the formation of the Ru(II)-carbene intermediate **C2** is kinetically more preferable than direct reductive migration to yield the final *trans*-addition product **B1**.

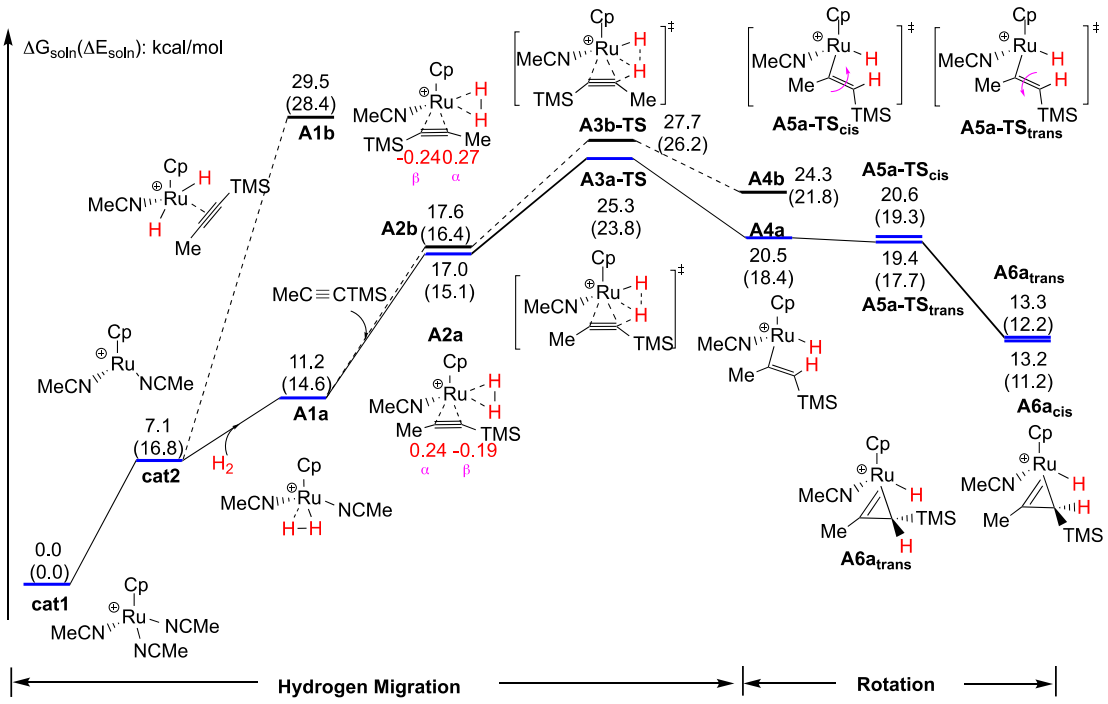

Figure 2. Energetic profiles of the most favorable pathway for the initial stage of the *gem*-hydrogenation in solution computed by the SMD M06 method.[15d]

Scheme 3. Energetic Profiles (kcal/mol) for Different Reductive Hydrogen Migration Pathways from the Two Ruthenacyclopropene Intermediates in Solution Computed by the SMD M06 Method.

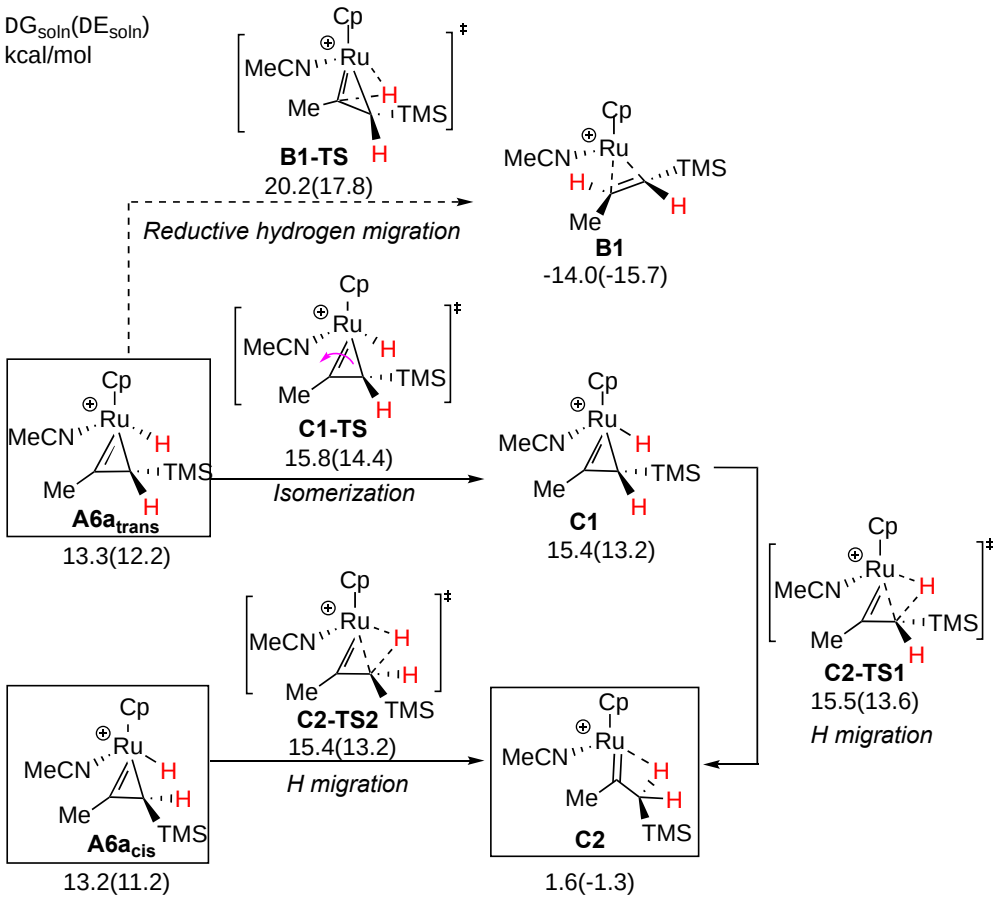

Next, the five-coordinate Ru(II)-carbene intermediate **C2** can bifurcate into two pathways (Figure 3). One possibility is the coordination of a MeCN ligand to form a stable six-coordinate Ru(II)-carbene **C3** (ΔG_{soln} = -6.2 kcal/mol), followed by an unusual 1,2-silyl migration from the C_β atom to the C_α atom (via **C3-TSa**; ΔG_{soln} = 10.7 kcal/mol) to form the desired *gem*-addition product **C4a**. Another competitive pathway, as suggested by the Fürstner and Thiel groups,[5c-d] involves coordination of another hydrogen molecule to **C2**. Subsequent oxidative addition via **D1-TS** proceeds to give a Ru(IV)-carbene dihydride intermediate **D2** (ΔG_{soln} = 10.6 kcal/mol).[15e] Next, one hydride migrates to the C_α atom of the carbene via **D2-TS** (ΔG_{soln} = 11.4 kcal/mol)

to afford the α-H agostic ruthenium(IV)-alkyl hydride intermediate **D3** and, subsequently, its β-H agostic isomer **D4** (Figure 3). Finally, β-H elimination of **D4** gives the *trans*-addition product **D5**. Moreover, other pathways involving 1,2-hydrogen migration to the C_α atom via **C3-TSb** (ΔG_{soln} = 28.0 kcal/mol) or β-hydride elimination via **C4-TSa** (21.9 kcal/mol) or **C4-TS2a** (17.6 kcal/mol) should be excluded due to their higher barriers. Furthermore, other possible mechanisms for the *gem*-addition, such as (1) the formation of metal-vinylidene intermediate (Scheme 4)[16] and (2) hydrogenation followed by β-Si elimination and hydrosilylation (see Figure S1 in the SI for details), were also found to have much higher reaction barriers (32.6 and 34.3 kcal/mol, respectively), and should be excluded. Overall, the *gem*-addition pathway depicted in Figure 3 was computed to be the most kinetically favorable pathway and had a slightly lower barrier than the *trans*-addition pathway by about 0.7 kcal/mol. This is qualitatively consistent with the observed low *gem*-selectivity when TMS-alkyne was used (Table 1, entry 4).

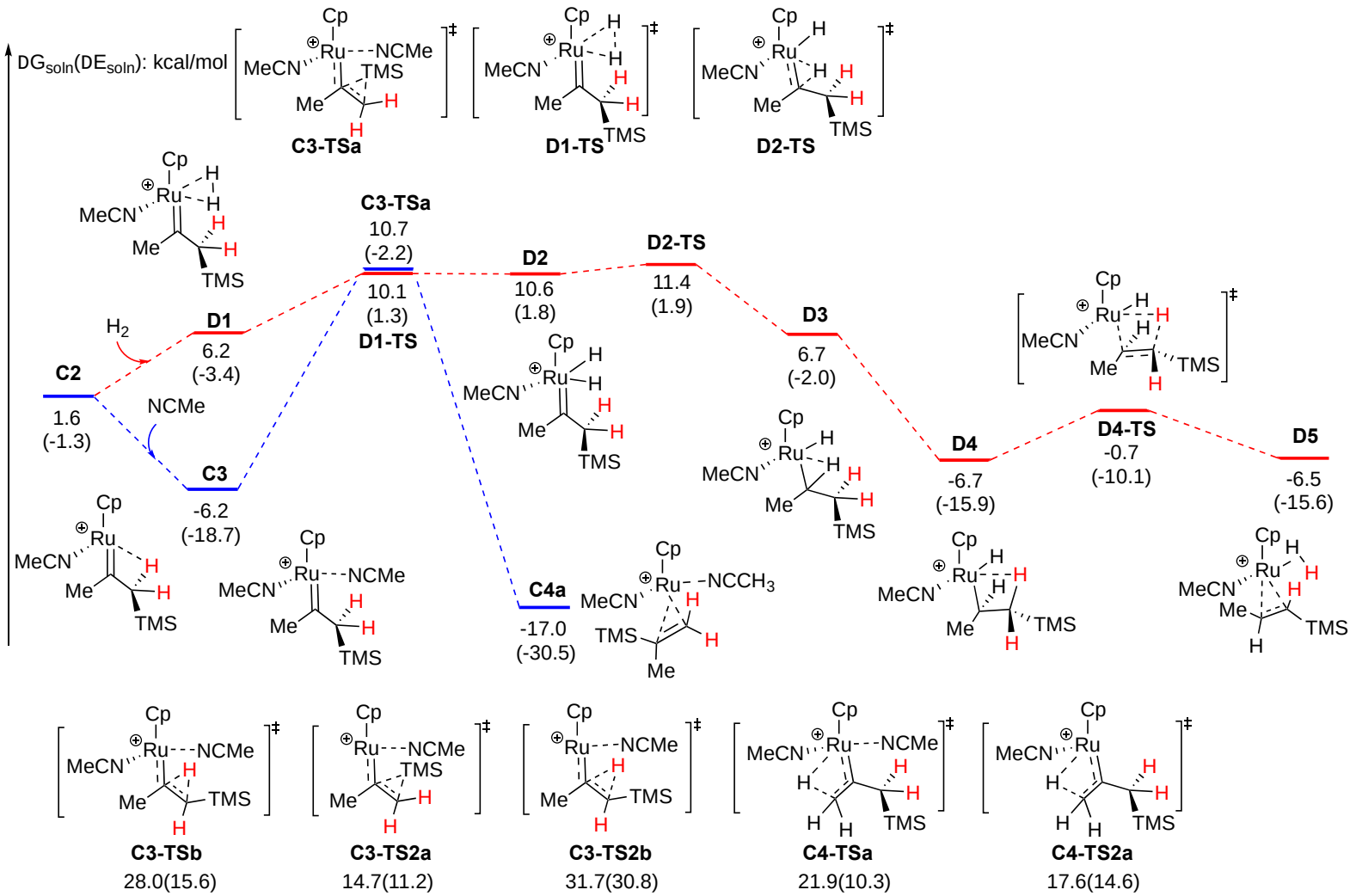

Figure 3. Energetic profiles of the most favorable pathway for the *gem*- and *trans*-addition hydrogenation in solution computed by the SMD M06 method.[15e]

Scheme 4. Energetic Profiles for the Metal Vinylidene Mechanism in Solution Computed by the SMD M06 Method.

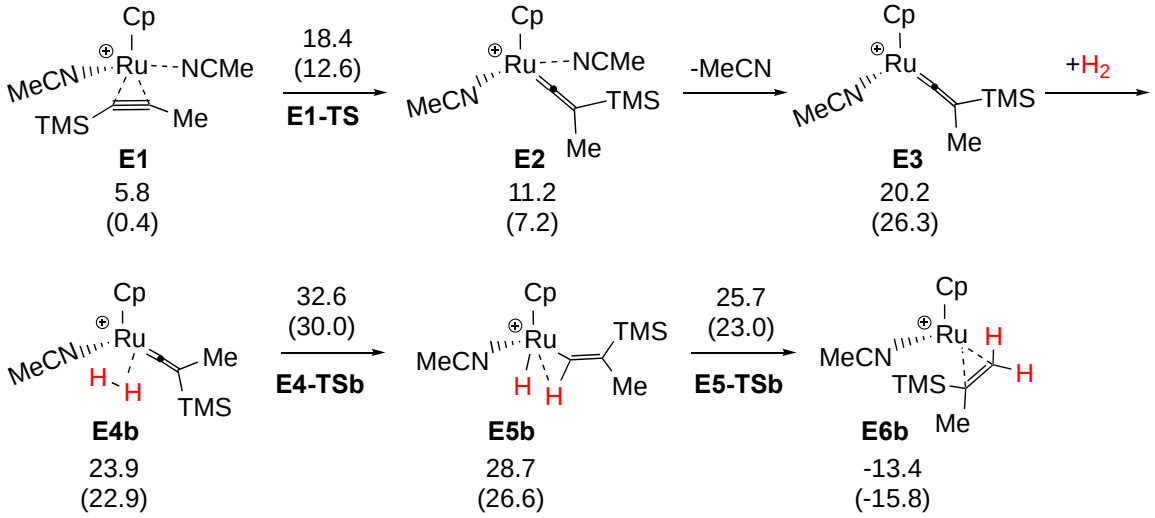

The important role of the phenyl group in $PhMe_2Si$- on the *gem*-addition was further examined by DFT calculations. When the $PhMe_2Si$-alkyne substrate was used, the higher computed selectivity (4.1 kcal/mol) towards *gem*-addition over *trans*-addition was also observed, compared to TMS-alkyne (0.7 kcal/mol, see Table 6 and Figure 4). In the key and favorable silyl migration step via **C3-TSa(SiPhMe$_2$)**, dissociation of one CH_3CN ligand and η^2-Ph coordination from $PhMe_2Si$ to the ruthenium center are involved, which has a lower barrier than the silyl migration step without the CH_3CN dissociation and phenyl coordination (via **C3-TS(SiPhMe$_2$)**, Figure 4) by about 4.9 kcal/mol. Hence, such phenyl coordination enhances *gem*-addition selectivity. On the other hand, when one small MeCN ligand was replaced by a bulkier DABCO ligand, the computed selectivity was reversed to prefer *trans*-addition by 4.0 kcal/mol (Table 6). Our results showed that the silyl migration step, in which the silyl group approached M=C_α site and the phenyl coordination to the metal was involved, was found to experience considerable steric repulsion with the bulky DABCO ligand and thus considerably raise the reaction barrier (Figure

4). These computational results are qualitatively consistent with the higher *gem*-selectivity by using the $PhMe_2Si$-substituted alkyne and with the reverse selectivity by the DABCO additive.

Table 6. Computed Relative Free Energies (kcal/mol) of the Key Transition States for the *trans*-addition and *gem*-addition Pathways with Different Alkynes (MeC≡C-*Si*) or Ligand (L) of the Catalyst in solution by the SMD M06 Method.

	***trans*-addition**			***gem*-addition**	***Selectivity***
Si/L	**B1-TS**	**D1-TS**	**D2-TS**	**C3-TS**	**$\Delta\Delta G^a$**
***Si* = TMS**	20.2	10.1	11.4	10.7	0.7
***Si* = $PhMe_2Si$**	21.8	10.1	10.7	6.6	4.1
L = DABCO[b]	26.4	–	15.6[c]	19.6	−4.0

[a]$\Delta\Delta G = \Delta G_{trans\text{-}add} - \Delta G_{gem\text{-}add}$. [b]The relative free energies are with respect to the $[CpRu(MeCN)_2(DABCO)]^+$ complex and isolated reactants. [c]Oxidative addition of H_2 concerted with hydrogen migration.

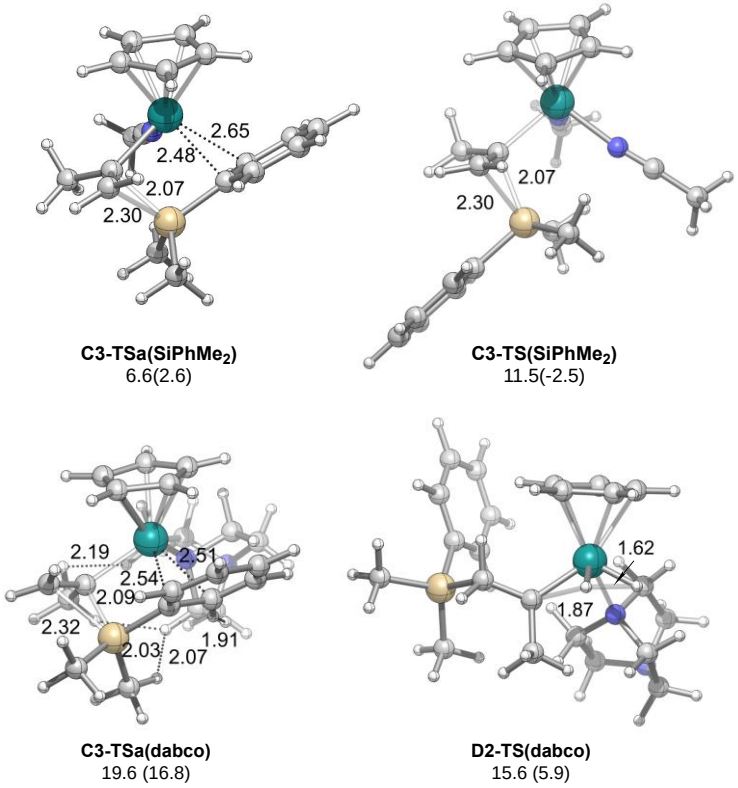

Figure 4. Computed geometries and relative free energies and electronic energies (in parenthesis) of the critical silyl migration step for the *gem*-addition with the MeC≡C-SiPhMe$_2$ substrate in solution by the SMD M06 method.

On the basis of the above DFT study, the overall mechanistic details of the unusual *gem*- and *trans*-hydrogenation are summarized in Scheme 5. The Ru(II)-carbene was found to be the key intermediate in these reactions. Depending on the ligand environment, the migration propensity of the silyl (vs. H) and H_2 pressure, this carbene intermediate can undergo either the unusual 1,2-silyl migration to give the *gem*-addition product (pathway B) or a cascade process involving oxidative addition of another H_2 followed by 1,2-hydrogen migration and β-H elimination to give the *trans*-addition product (pathway A). The *gem*-addition can be enhanced by a phenyl substituent on the silyl group through coordination to the ruthenium center in the key silyl migration step. The pathway A is consistent with Fürstner's observation.[5] In retrospect, the observed inverse dependence of the B/L ratio on hydrogen pressure was also consistent with the proposed pathways, as pathway A should be more favored at high pressure due to the involvement of another hydrogen molecule.

Scheme 5. Proposed Mechanisms for Ru-Catalyzed *gem*- and *trans*-Hydrogenation.

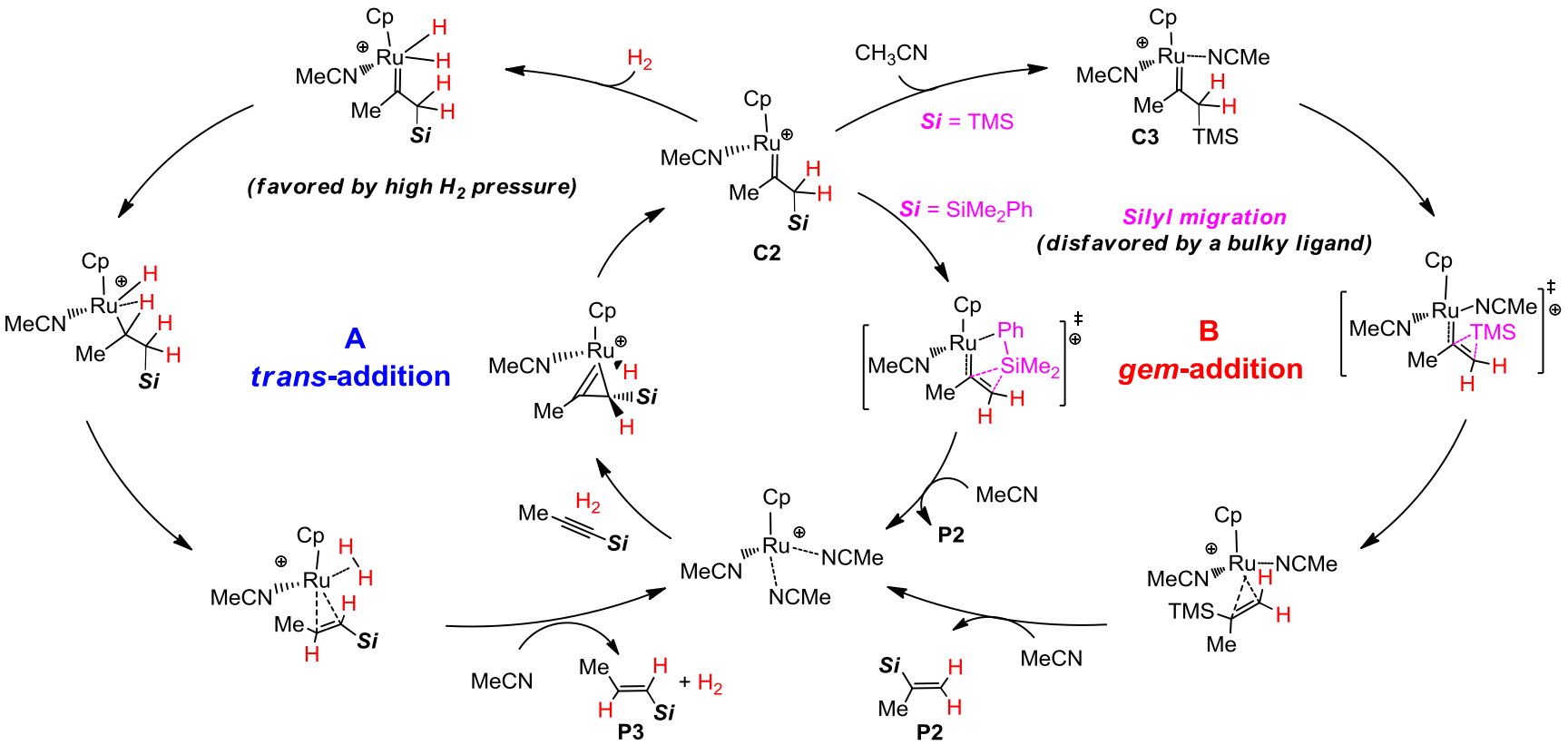

Control Experiments. More experiments were designed to further substantiate the proposed mechanism for the unusual *gem*-hydrogenation, particularly to differentiate the Ru-carbene pathway (**C3** in Scheme 5) from the silyl-migrated Ru-vinylidene pathway (**B3** in Scheme 4), as the latter intermediate has been widely known with Ru-catalytic systems for internal alkynes.[16] Thus, we designed two alkynes bearing two different silyl groups (**4** and **5**). If the Ru-vinylidene intermediate is involved, alkyne **4** will proceed to form **VD-4** only, while alkyne **5** will form **VD-5** only (Scheme 6). These two different vinylidene intermediates should proceed separately to form the two corresponding hydrogenation products **6** and **7**, respectively. However, if the *gem*-H_2 Ru-carbene intermediate is operative, these two alkynes should proceed to form the same intermediate **CB**. Subsequent silyl migration would lead to a mixture of two products (both **6** and **7**) resulting from silyl migrations from both sides, and theoretically, the ratios of the two products from the two alkynes should be equal as a result of the common intermediate. In fact, when the two alkynes were subjected separately to the standard *gem*-hydrogenation conditions, both **6** and **7** were formed as a mixture. The ratios between **6** and **7** from both alkynes were essentially the same (Scheme 6). Therefore, these observations provided a concrete discrimination of the two mechanisms and excluded the involvement of the Ru-vinylidene intermediate. They are also consistent with our DFT calculations (Scheme 5) as well as the observations by Fürstner.[5]

Scheme 6. Experimental Differentiation between Ru-Vinylidene and *gem*-H_2 Ru-Carbene Intermediates.

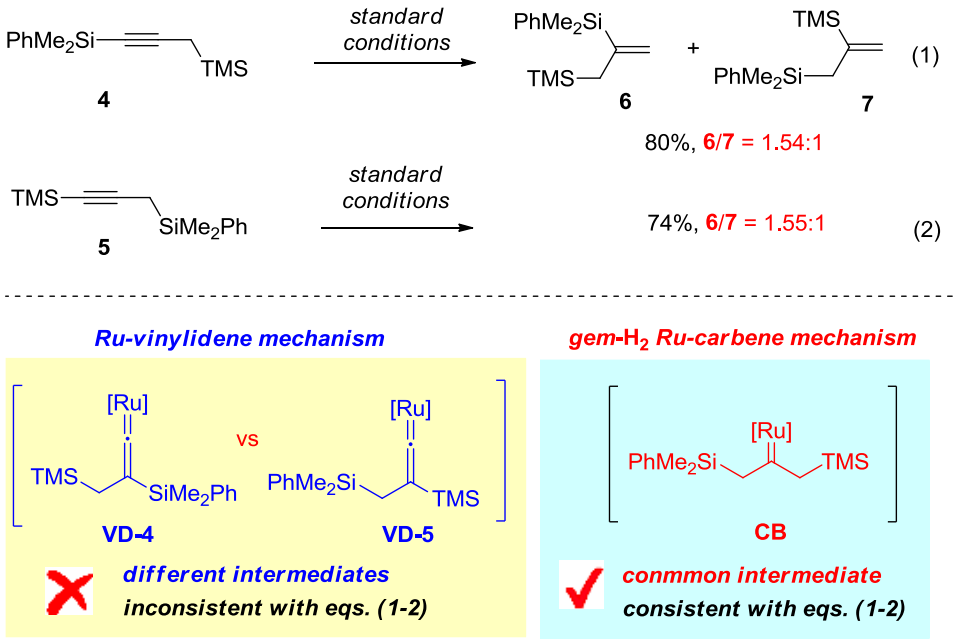

Furthermore, silyl migration sometimes occurs by dissociation to form a silyl cation followed by recombination. In order to probe this possibility, a cross-over experiment was designed (Scheme 7). Under the standard conditions, a mixture of alkynes **1q** and **8** reacted to form the corresponding products **2q** and **9** in high yields. The cross-over products **9** and **10** were not observed, which excluded the possibility of fragmentation to form silyl cations in this process.

Scheme 7. A Cross-over Experiment to Probe Possible Involvement of Silyl Cations

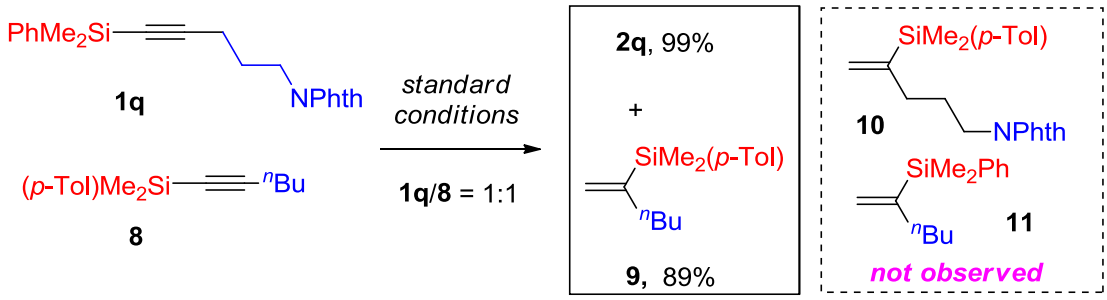

Furthermore, based on our computational conclusion, the two hydrogen atoms for the *gem*-hydrogenation should originate from the same H_2 molecule, while they can come from two different H_2 molecules for the *trans*-hydrogenation. We then carried out cross-over experiments using a mixture of H_2/D_2 (Scheme 8). When alkyne **1h** was subjected to the *gem*-hydrogenation conditions, the corresponding products **2h**-d_2 and **2h** were formed, but no cross-over product **2h**-d_1 (with H–D scrambling) was observed. However, when the *trans*-hydrogenation conditions were employed, the reaction of **1y** in mixed H_2/D_2 atmosphere formed not only **3y** and **3y**-d_2, but also the cross-over product **3y**-d_1. These experimental results further supported our calculated favorable pathways for both *gem*- and *trans*-hydrogenation summarized in Scheme 5.[17]

Scheme 8. Cross-over Experiments with H_2/D_2.

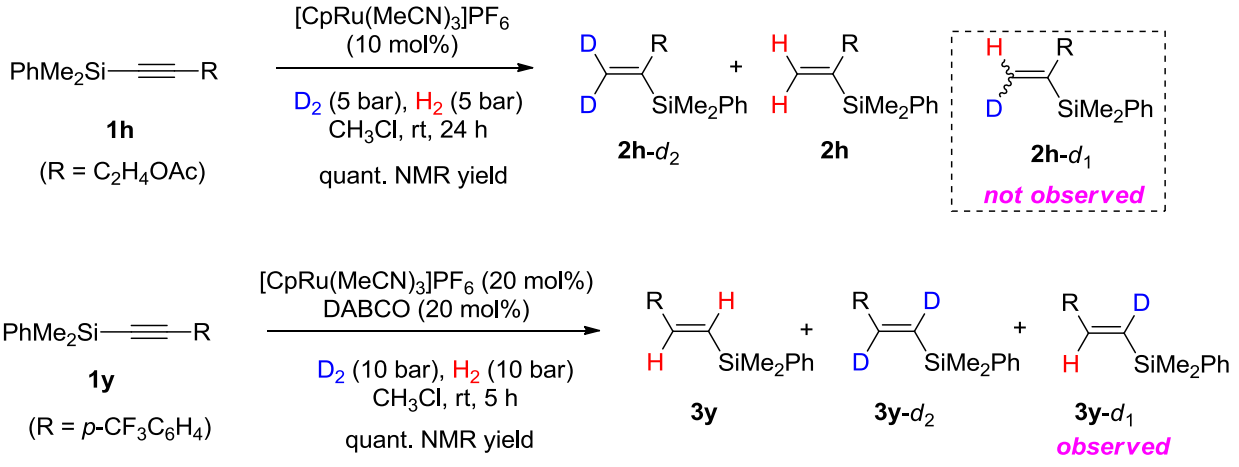

Conclusion

We have developed the first migratory geminal semi-hydrogenation of silyl alkynes. This process not only provides new access to the useful terminal vinylsilanes, but also presents a new mode of reactivity of silyl alkynes, which is complementary to the established *cis*- and *trans*-semi-hydrogenation. Different from the previously preferred [Cp*Ru]-based system for *trans*-hydrogenation of alkynes, the use of [CpRu]-based system was found to be superior in this unusual hydrogenation reaction. With the proper choice of a silyl group and suitable tuning of the cationic nature of the catalyst, both aryl- and alkyl-substituted silyl alkynes can participate in this highly efficient and *gem*-selective process. With a suitable additive (i.e., DABCO), we were also able to alter the selectivity to favor *trans*-hydrogenation for aryl alkynes with good selectivity. DFT computations provided important insights into the mechanisms for both *gem*- and *trans*-selectivity. The superior role of the phenyldimethylsilyl group in the uncommon silyl migration was also rationalized. Moreover, the *gem*-H_2 Ru-carbene intermediate was proposed to be the key intermediate for both *gem*- and *trans*-hydrogenation, rather than the Ru-vinylidene intermediate, which was also substantiated by experimental results. The delicate design of two disilyl alkynes provided concrete evidence for the differentiation of these two pathways. The uncommon *gem*-addition[5] and/or silyl migration from C_β in the metal-carbene intermediate should open up a new synthetic avenue for alkyne transformations.

ASSOCIATED CONTENT

Supporting Information

The Supporting Information is available free of charge via the Internet at http://pubs.acs.org at DOI: .

Experimental and computational details and NMR data (PDF).

AUTHOR INFORMATION

Corresponding Author

*J.S.: sunjw@ust.hk

*L.W.C.: oscarchung@sustech.edu.cn

ORCID

Jianwei Sun: 0000-0002-2470-1077

Lung Wa Chung: 0000-0001-9460-7812

Xinhao Zhang: 0000-0002-8210-2531

Yun-Dong Wu: 0000-0003-4477-7332

Author Contributions

‡ L.S. and Q.F. contributed equally to the work. L.S. contributed to the computational part, and Q.F. contributed to the experimental part.

Notes

The authors declare no competing financial interest.

Acknowledgment: We thank Dr. Tao Zhang for experimental assistance and Haonan Wu for computational assistance. We gratefully acknowledge the financial support from the National Natural Science Foundation of China (21572192, 21490570, 21672096, 21702095, 21933004) and Shenzhen Science and Technology Innovation Committee (JCYJ20170818113708560, JCYJ20170412150507046, JCYJ20170412150343516, JCYJ20160229205441091) the Shenzhen Nobel Prize Scientists Laboratory Project (C17783101), and the Shenzhen San-Ming Project (SZSM201809085). L.S. also thanks the Humboldt Foundation for the financial support.

References

(1) Reviews of semi-hydrogenation of alkynes: (a) Michaelides, I. N.; Dixon, D. J. Catalytic Stereoselective Semihydrogenation of Alkynes to *E*-Alkenes. *Angew. Chem., Int. Ed.* **2013**, *52*, 806−808. (b) Kluwer, A. M.; Elsevier, C. J. In *The Handbook of Homogeneous Hydrogenation*; de Vries, J. G., Elsevier, C. J., Eds., Wiley-VCH: Weinheim, 2007; Vol. 1; pp 375−411. (c) Pasto, D. J. In *Comprehensive Organic Synthesis*; Trost, B. M., Fleming I., Eds., Pergamon: Oxford, 1991; Vol. 8; pp 471−488.

(2) (a) Lindlar, H. A new catalyst for selective hydrogenation. *Helv. Chim. Acta* **1952**, *35*, 446−450. (b) Lindlar, H.; Dubuis, R. Palladium Catalyst for Partial Reduction of Acetylenes. *Org. Synth.* **1966**, *46*, 89. (c) Schrock, R. R.; Osborn, J. A. Catalytic Hydrogenation Using Cationic Rhodium Complexes. II. The Selective Hydrogenation of Alkynes to *Cis* Olefins. *J. Am. Chem. Soc.* **1976**, *98*, 2143−2147. (d) Choudary, B. M.; Vasantha, G.; Sharma, M.; P. Bharathi, A Highly Selective Montmorillonite Catalyst for Hydrogenation of Alkynes, Alkenynes, and Alkadienes. *Angew. Chem., Int. Ed.* **1989**, *28*, 465−466. (e) van Laren, M. W.; Elsevier, C. J. Selective Homogeneous Palladium(0)-Catalyzed Hydrogenation of Alkynes to

(*Z*)-Alkenes. *Angew. Chem., Int. Ed.* **1999**, *38*, 3715−3717. (f) Chernichenko, K.; Madarász, Á.; Papai, I.; Nieger, M.; Leskelä, M.; Repo, T. A frustrated-Lewis-pair approach to catalytic reduction of alkynes to *cis*-alkenes. *Nat. Chem.* **2013**, *5*, 718−723. (g) Semba, K.; Kameyama, R.; Nakao, Y. Copper-Catalyzed Semihydrogenation of Alkynes to Z-Alkenes. *Synlett* **2015**, *26*, 318−322. (h) Wakamatsu, T.; Nagao, K.; Ohmiya, H.; Sawamura, M. Copper-Catalyzed Semihydrogenation of Internal Alkynes with Molecular Hydrogen. *Organometallics* **2016**, *35*, 1354−1357. (i) Das, M.; Kaicharla, T.; Teichert, J. F. Stereoselective Alkyne Hydrohalogenation by Trapping of Transfer Hydrogenation Intermediates. *Org. Lett.* **2018**, *20*, 4926−4929.

(3) (a) Burch, R. R.; Muetterties, E. L.; Teller, R. G.; Williams, J. M. Selective Formation of *Trans* Olefins by a Catalytic Hydrogenation of Alkynes Mediated at Two Adjacent Metal Centers. *J. Am. Chem. Soc.* **1982**, *104*, 4257−4258. (b) Schleyer, D.; Niessen, H. G.; Bargon, J. In situ ^{1}H-PHIP-NMR studies of the stereoselective hydrogenation of alkynes to (*E*)-alkenes catalyzed by a homogeneous $[Cp^*Ru]^+$ catalyst. *New J. Chem.* **2001**, 25, 423−426. (c) Srimani, D.; Diskin-Posner, Y.; Ben-David, Y.; Milstein, D. Iron Pincer Complex Catalyzed, Environmentally Benign, *E*-Selective Semi-Hydrogenation of Alkynes. *Angew. Chem., Int. Ed.* **2013**, *52*, 14131−14134. (d) Karunananda, M. K.; Mankad, N. P. *E*-Selective Semi-Hydrogenation of Alkynes by Heterobimetallic Catalysis. *J. Am. Chem. Soc.* **2015**, *137*, 14598−14601. (e) Tokmic, K.; Fout, A. R. Alkyne Semihydrogenation with a Well-Defined Nonclassical Co−H_2 Catalyst: A H_2 Spin on Isomerization and *E*-Selectivity. *J. Am. Chem. Soc.* **2016**, *138*, 13700−13705. (f) Furukawa, S.; Komatsu, T. Selective Hydrogenation of Functionalized Alkynes to (*E*)-Alkenes, Using Ordered Alloys as Catalysts. *ACS Catal.* **2016**, *6*, 2121−2125.

(4) (a) Trost, B. M.; Ball, Z. T.; Jöge, T. A Chemoselective Reduction of Alkynes to (*E*)-Alkenes. *J. Am. Chem. Soc.* **2002**, *124*, 7922−7923. (b) Fürstner, A.; Radkowski, K. A chemo- and stereoselective reduction of cycloalkynes to (*E*)-cycloalkenes. *Chem. Commun.* **2002**, 2182−2183. (c) Trost, B. M.; Ball, Z. T. Alkyne Hydrosilylation Catalyzed by a Cationic Ruthenium Complex: Efficient and General *Trans* Addition. *J. Am. Chem. Soc.* **2005**, *127*, 17644−17655. (d) Micoine, K.; Fürstner, A. Concise Total Synthesis of the Potent Translation and Cell Migration Inhibitor Lactimidomycin. *J. Am. Chem. Soc.* **2010**, *132*, 14064−14066. (e) Micoine, K.; Persich, P.; Llaveria, J.; Lam, M.-H.; Maderna, A.; Loganzo, F.; Fürstner, A. Total Syntheses and Biological Reassessment of Lactimidomycin, Isomigrastatin and Congener Glutarimide Antibiotics. *Chem.-Eur. J.* **2013**, *19*, 7370−7383. (f) Frihed, T. G.; Fürstner, A. Progress in the *trans*-Reduction and *trans*-Hydrometalation of Internal Alkynes. Applications to Natural Product Synthesis. *Bull. Chem. Soc. Jpn.* **2016,** *89*, 135−160. (g) Mata, G.; Wölfl, B.; Fürsnter, A. Synthesis and Molecular Editing of Callyspongiolide, Part 1: The Alkyne Metathesis/*trans*-Reduction Strategy. *Chem.-Eur. J.* **2019**, *25*, 246−254.

(5) (a) Radkowski, K., Sundararaju, B.; Fürstner, A. A functional-group-tolerant catalytic *trans* hydrogenation of alkynes. *Angew. Chem., Int. Ed.* **2013**, *52*, 355−360. (b) Fuchs, M.; Fürstner, A. *trans*-Hydrogenation: Application to a Concise and Scalable Synthesis of Brefeldin A. *Angew. Chem., Int. Ed.* **2015**, *54*, 3978−3982. (c) Leutzsch, M.; Wolf, M. L.; Gupta, P.; Fuchs, M.; Thiel, W.; Farès, C.; Fürstner, A. Formation of Ruthenium Carbenes by *gem*-Hydrogen Transfer to Internal Alkynes: Implications for Alkyne *trans*-Hydrogenation. *Angew. Chem., Int. Ed.* **2015**, *54*, 12431−12436. (d) Guthertz, A.; Leutzsch, M.; Wolf, L. M.; Gupta, P.; Rummelt, S. M.; Goddard, R.; Farès, C.; Thiel, W.; Fürstner, A. Half-Sandwich Ruthenium Carbene Complexes Link *trans*-Hydrogenation and gem-

Hydrogenation of Internal Alkynes. *J. Am. Chem. Soc.* **2018,** *140*, 3156−3169. (e) Fürstner, A. *trans*-Hydrogenation, *gem*-Hydrogenation, and *trans*-Hydrometalation of Alkynes: An Interim Report on an Unorthodox Reactivity Paradigm. *J. Am. Chem. Soc.* **2019**, *141*, 11−24. (f) Biberger, T.; Gordon, C. P. Leutzsch, M.; Peil, S.; Guthertz, A.; Copéret, C.; Fürstner, A. Alkyne *gem*-Hydrogenation: Formation of Pianostool Ruthenium Carbene Complexes and Analysis of Their Chemical Character. *Angew. Chem., Int. Ed.* **2019**, *58*, 8845−8850.

(6) Our efforts: (a) Ding, S.; Song, L.-J.; Chung, L. W.; Zhang, X.; Sun, J.; Wu, Y.-D. Ligand-Controlled Remarkable Regio- and Stereodivergence in Intermolecular Hydrosilylation of Internal Alkynes: Experimental and Theoretical Studies. *J. Am. Chem. Soc.* **2013**, *135*, 13835−13842. (b) Song, L.-J.; Ding, S.; Wang, Y.; Zhang, X.; Wu, Y.-D.; Sun, J. Ir-Catalyzed Regio- and Stereoselective Hydrosilylation of Internal Thioalkynes: A Combined Experimental and Computational Study. *J. Org. Chem.* **2016**, *81*, 6157−6164. (c) Ding, S.; Song, L.-J.; Wang, Y.; Zhang, X.; Chung, L. W.; Wu, Y.-D.; Sun, J. Highly Regio- and Stereoselective Hydrosilylation of Internal Thioalkynes under Mild Conditions. *Angew. Chem., Int. Ed.* **2015**, *54*, 5632−5635.

(7) Utility of silyl alkynes: (a) Larson, G. L. Some Aspects of the Chemistry of Alkynylsilanes. *Synthesis* **2018**, *50*, 2433−2462. (b) Lozanov, M.; Montgomery, J. Nickel-catalyzed preparation of stereodefined allylic alcohols using silicon-tethered ynals. *Tetrahedron Lett.* **2001**, *42*, 3259−3261. (c) O'Neil, G. W.; Phillips, A. J. Total Synthesis of (-)-Dictyostatin. *J. Am. Chem. Soc.* **2006**, *128*, 5340−5541.

(8) Utility of vinyl silanes: Ojima, I.; Li, Z.; Zhu, J. In *The Chemistry of Organosilicon Compounds*; Rappoport, S.; Apeloig, Y., Eds.; Wiley: New York, 1998. (b) Langkopf, E.;

Schinzer, D. Uses of Silicon-Containing Compounds in the Synthesis of Natural Products. *Chem. Rev.* **1995**, *95*, 1375−1406. (c) Trost, B. M.; Ball, Z. T.; Joge, T. Regioselective Hydrosilylation of Propargylic Alcohols: An Aldol Surrogate. *Angew. Chem., Int. Ed.* **2003**, *42*, 3415−3418. (d) Trost, B. M.; Ball, Z. T.; Laemmerhold, K. M. An Alkyne Hydrosilylation-Oxidation Strategy for the Selective Installation of Oxygen Functionality. *J. Am. Chem. Soc.* **2005**, *127*, 10028−10038.

(9) For selected examples of cationic $[Cp^*Ru(MeCN)_3]^+$ catalysis for alkyne additions: (a) Trost, B. M.; Ball, Z. T. Intramolecular Endo-Dig Hydrosilylation Catalyzed by Ruthenium: Evidence for a New Mechanistic Pathway. *J. Am. Chem. Soc.* **2003**, *125*, 30−31. (b) Sundararaju, B.; Fürstner, A. A *trans*-Selective Hydroboration of Internal Alkynes. *Angew. Chem., Int. Ed.* **2013**, *52*, 14050−14054. (c) Rummelt, S. M.; Fürstner, A. Ruthenium-Catalyzed *trans*-Selective Hydrostannation of Alkynes. *Angew. Chem., Int. Ed.* **2014**, *53*, 3626−3630. (d) Rummelt, S. M.; Radkowski, K.; Roşca, D.-A.; Fürstner, A. Interligand Interactions Dictate the Regioselectivity of *trans*-Hydrometalations and Related Reactions Catalyzed by [Cp*RuCl]. Hydrogen Bonding to a Chloride Ligand as a Steering Principle in Catalysis. *J. Am. Chem. Soc.* **2015**, *137*, 5506−5519.

(10) Examples of other [Cp*Ru]-based catalysis: (a) Roşca, D.-A.; Radkowski, K.; Wolf, L. M.; Wagh, M.; Goddard, R.; Thiel, W.; Fürstner, A. Ruthenium-Catalyzed Alkyne *trans*-Hydrometalation: Mechanistic Insights and Preparative Implications. *J. Am. Chem. Soc.* **2017**, *139*, 2443−2455. (b) Rummelt, S. M.; Cheng, G.-J.; Gupta, P.; Thiel, W.; Fürstner, A. Hydroxy-Directed Ruthenium-Catalyzed Alkene/Alkyne Coupling: Increased Scope, Stereochemical Implications, and Mechanistic Rationale. *Angew. Chem., Int. Ed.* **2017**, *56*, 3599−3604; Corrigendum: **2017**, *56*, 5652.

(11) For selected examples with cationic $[CpRu(MeCN)_3]^+$ catalysis: (a) Trost, B. M.; Rudd, M. T. An Unusual Ruthenium-Catalyzed Dimerization of Propargyl Alcohols. *J. Am. Chem. Soc.* **2001**, *123*, 8862−8863. (b) Trost, B. M.; Ball, Z. T. Markovnikov Alkyne Hydrosilylation Catalyzed by Ruthenium Complexes. *J. Am. Chem. Soc.* **2001**, *123*, 12726−12727. (c) Trost, B. M.; Cregg, J. J. Ruthenium-Catalyzed Alkene−Alkyne Coupling of Disubstituted Olefins: Application to the Stereoselective Synthesis of Trisubstituted Enecarbamates. *J. Am. Chem. Soc.* **2015**, *137*, 620−623. (d) Trost, B. M.; Toste, F. D.; Pinkerton, A. B. Non-Metathesis Ruthenium-Catalyzed C-C Bond Formation. *Chem. Rev.* **2001**, *101*, 2067−2096.

(12) (a) Anderson, J. C.; Munday, R. H. Vinyldimethylphenylsilanes as Safety Catch Silanols in Fluoride-Free Palladium-Catalyzed Cross-Coupling Reactions. *J. Org. Chem.* **2004**, *69*, 8971−8974. (b) Fleming, I.; Henning, R.; Parker, D. C.; Plaut, H. E.; Sanderson, P. E. J. The Phenyldimethylsilyl Group as a Masked Hydroxy Group. *J. Chem. Soc., Perkin Trans. 1* **1995**, 317−337.

(13) (a) Chung, L. W.; Wu, Y.-D.; Trost, B. M.; Ball, Z. T. A Theoretical Study on the Mechanism, Regiochemistry, and Stereochemistry of Hydrosilylation Catalyzed by Cationic Ruthenium Complexes. *J. Am. Chem. Soc.* **2003**, *125*, 11578−11582. (b) Song, L.-J.; Wang, T.; Zhang, X.; Chung, L. W.; Wu, Y.-D. A Combined DFT/IM-MS Study on the Reaction Mechanism of Cationic Ru(II)-Catalyzed Hydroboration of Alkynes. *ACS Catal.* **2017**, *7*, 1361−1368. (c) Selected recent computational studies of metal-catalyzed hydrogenation reaction: Rosales, A. R.; Wahlers, J.; Limé, E.; Meadows, R. E.; Leslie, K. W.; Savin, R.; Bell, F.; Hansen, E. Helquist, P.; Munday, R. H.; Wiest, O.; Norrby, P.-O. Rapid virtual screening of enantioselective catalysts using CatVS. *Nat. Catal.* **2019**, *2*,

41−45. (d) Zhang, Y.; Roberts, S. P.; Bergman, R. G.; Ess, D. H. Mechanism and Catalytic Impact of Ir–Ta Heterobimetallic and Ir–P Transition Metal/Main Group Interactions on Alkene Hydrogenation. *ACS Catal.* **2015**, *5*, 1840−1849. (e) Qu, S.; Dai, H.; Dang, Y.; Song, C.; Wang, Z.-X.; Guan, H. Computational Mechanistic Study of Fe-Catalyzed Hydrogenation of Esters to Alcohols: Improving Catalysis by Accelerating Precatalyst Activation with a Lewis Base. *ACS Catal.* **2014**, *4*, 4377−4388. (f) Takagi, N.; Sakaki, S. Theoretical Study of Reactivity of Ge(II)-hydride Compound: Comparison with Rh(I)-Hydride Complex and Prediction of Full Catalytic Cycle by Ge(II)-hydride. *J. Am. Chem. Soc.* **2013**, *135*, 8955−8965. (g) Wu, S.-B.; Zhang, T.; Chung, L. W.; Wu, Y.-D. A Missing Piece of the Mechanism in Metal-Catalyzed Hydrogenation: Co(−I)/Co(0)/Co(+I) Catalytic Cycle for Co(−I)-Catalyzed Hydrogenation. *Org. Lett.* **2019**, *21*, 360−364.

(14) The preference for the oxidative hydrogen migration to C_β via **A3a-TS** to form **A4a** over the related migration via **A3b-TS** to form **A4b** can be attributed to the charge distribution of the silyl alkyne in **A2a** and **A2b** C_α–C_β (Mulliken charge for C_β (-0.19~-0.24) and C_α (0.23-0.27)). Therefore, the proton character in the oxidative hydrogen migration makes it preferentially transfer to the more electron-rich C_β in **A2a**. In addition, **A4a** is more stable than **A4b**, in which the methyl group was further suggested to have a stronger donating ability than the silyl group. In hydrosilylation, hydrogen migration to C_β was also preferred for less steric repulsion (ref. 6a).

(15) (a) Tanke, R. S.; Crabtree, R. H. Unusual activity and selectivity in alkyne hydrosilylation with an iridium catalyst stabilized by an oxygen-donor ligand. *J. Am. Chem. Soc.* **1990,** *112*, 7984−7989. (b) Casey, C. P.; Brady, J. T.; Boller, T. M.; Weinhold, F.; Hayashi, R. K. Protonation of Rhenium Alkyne Complexes Produces η^3-Allyl Rhenium Complexes via

Observable 1-Metallacyclopropene Intermediates. *J. Am. Chem. Soc.* **1998,** *120*, 12500−12511. (c) Bernal, M. J.; Torres, O.; Martín, M.; Sola, E. Reversible Insertion of Carbenes into Ruthenium–Silicon Bonds. *J. Am. Chem. Soc.* **2013,** *135*, 19008−19015. (d) **A4a** was computed to be 1.1 kcal/mol higher in free energy than **A5a-TS$_{trans}$** due to the ZPE and free energy correction. The former one is lower in electronic energy without the ZPE correction than the latter one by 0.5 kcal/mol. As **A4a** is very similar in energy to **A5a-TS$_{trans}$**, the oxidative hydrogen migration step might be considered to be concerted with the C–C bond rotation to directly form the ruthenacyclopropene intermediate **A6a$_{trans}$**. (e) Similar energy order switching due to the abovementioned ZPE and free energy correction was also found in **D1-TS** and **D2** (Figure 3).

(16) For a review and selected examples of Ru-vinylidene intermediates: (a) Bruneau, C.; Dixneuf, P. H. *Metal Vinylidenes and Allenylidenes in Catalysis: From Reactivity to Applications in Synthesis*; Wiley-VCH: Weinheim, 2008. (b) Trost, B. M.; McClory, A. Metal Vinylidenes as Catalytic Species in Organic Reactions. *Chem. Asian J.* **2008**, *3*, 164−194. (c) Huang, D.; Folting, K.; Caulton, K. G. Silyl Migration of $Me_3SiCCPh$ Coordinated to $[RuH(CO)(P^tBu_2Me)_2]BAr'_4$ Can Be Reversed: Synthesis and Structure of $[Ru(CH=C(SiMe_3)(Ph))(CO)(P^tBu_2Me)_2]BAr'_4$. *J. Am. Chem. Soc.* **1999**, *121*, 10318−10322. (d) Otsuka, M.; Tsuchida, N.; Ikeda, Y.; Kimura, Y.; Mutoh, Y.; Ishii, Y.; Takano, K. DFT Study of Internal Alkyne-to-Disubstituted Vinylidene Isomerization in $[CpRu(PhC{\equiv}CAr)(dppe)]^+$. *J. Am. Chem. Soc.* **2012**, *134*, 17746−17756. (e) Watanabe, T.; Mutoh, Y.; Saito, S. Ruthenium-Catalyzed Cycloisomerization of 2-Alkynylanilides: Synthesis of 3-Substituted Indoles by 1,2-Carbon Migration. *J. Am. Chem. Soc.* **2017**, *139*, 7749−7752.

TOC Graphic

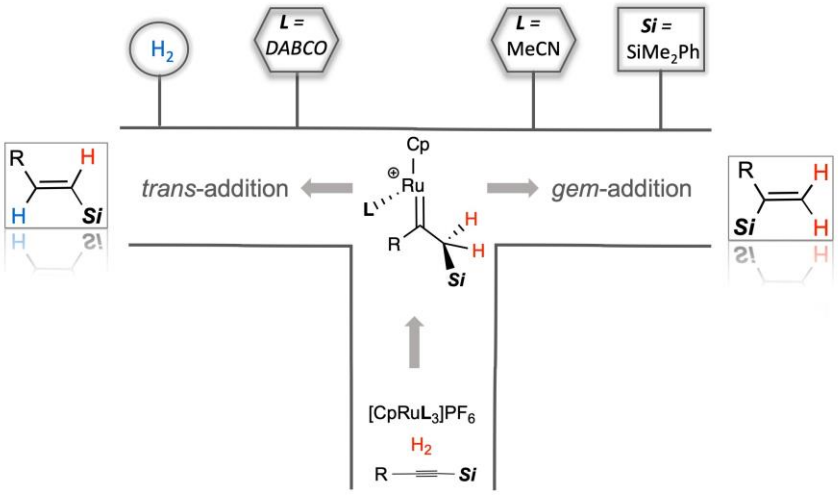
H2
L = DABCO
L = MeCN
Si = SiMe2Ph
trans-addition
gem-addition
Cp
Ru
L
R
H
H
Si
[CpRuL3]PF6
H2
R
Si